HHS Public Access

Author manuscript

Neurotoxicology. Author manuscript; available in PMC 2022 December 01.

Published in final edited form as:

Neurotoxicology. 2021 December ; 87: 94–105. doi:10.1016/j.neuro.2021.09.002.

YAC128 mouse model of Huntington disease is protected against subtle chronic manganese (Mn)-induced behavioral and neuropathological changes

Jordyn M. Wilcox[*,1,2], **Anna C. Pfalzer**[*,3], **Adriana A. Tienda**[1], **Ines F. Debbiche**[2], **Ellen C. Cox**[1], **Melissa S. Totten**[4], **Keith M. Erikson**[4], **Fiona E. Harrison**[1,2], **Aaron B. Bowman**[5]

[1]Division of Diabetes, Endocrinology and Metabolism, Department of Medicine, Vanderbilt University Medical Center, Nashville, TN

[2]Vanderbilt Brain Institute, Vanderbilt University, Nashville, TN

[3]Department of Neurology, Vanderbilt University Medical Center, Nashville, TN

[4]Department of Nutrition, University of North Carolina-Greensboro, Greensboro, NC

[5]School of Health Sciences, Purdue University, West Lafayette, IN

Abstract

Manganese (Mn) is an essential micronutrient but excessive levels induce neurotoxic effects. Increasing evidence suggests a deficit of bioavailable Mn in Huntington disease (HD), an inherited neurodegenerative disease characterized by motor and cognitive disturbances. Previous studies have shown rescue of some molecular HD phenotypes by acute Mn exposure. This study simultaneously examined the potential for chronic Mn exposure to attenuate HD behavioral phenotypes, and for the HD genotype to offer protection against detrimental effects of chronic Mn exposure. In two independent studies a chronic Mn exposure paradigm was implemented in the YAC128 mouse model of HD and behavior was assessed at several timepoints. Study 1 exposed WT and YAC128 mice to twice weekly subcutaneous injections of 0, 5, 15, or 50 mg/kg MnCl[2] tetrahydrate from 12-32 weeks of age. A promising protective effect against motor coordination decline in 5 mg/kg MnCl[2] tetrahydrate-treated YAC128 mice was detected. Study 2 thus exposed WT and YAC128 mice to either 0 or 5 mg/kg MnCl[2] tetrahydrate from 12-52 weeks of age (with a partial randomized treatment crossover at 31 weeks). The same protective effect was

[*]These authors contributed equally to this work.

CRediT author contributions

Jordyn M. Wilcox*: Conceptualization, Investigation, Methodology, Formal Analysis, Writing – Original Draft, Visualization **Anna C. Pfalzer*:** Conceptualization, Investigation, Methodology, Formal Analysis **Adriana A. Tienda:** Investigation **Ines F. Debbiche:** Investigation **Ellen C. Cox:** Investigation **Melissa S. Totten:** Investigation **Keith M. Erikson:** Investigation, Supervision **Fiona E. Harrison:** Conceptualization, Supervision, Writing – Review & Editing **Aaron B. Bowman:** Conceptualization, Supervision, Writing – Review & Editing, Funding Acquisition

All authors have read and approved the published version of the manuscript. *JMW and ACP contributed equally to this work.

Declaration of interests

The authors declare that they have no known competing financial interests or personal relationships that could have appeared to influence the work reported in this paper.

not observed under these conditions at higher statistical power. We report subtle toxicological changes in exploratory behavior and total activity induced by chronic Mn exposure in WT mice only, despite similar total increases in brain Mn in WT and YAC128 mice. Further, chronic Mn treatment resulted in a 10-12% decrease in striatal NeuN positive cell density in WT mice but not YAC128 mice, despite vehicle cell counts already being reduced compared to WT mice as expected for the HD genotype. The subtle changes observed in specific outcome measures, but not others, following long-term low-level Mn exposure in WT mice delineate the neurobehavioral and neuropathological effects at the threshold of chronic Mn toxicity. We conclude that these chronic low-dose Mn exposures do not significantly rescue behavioral HD phenotypes, but YAC2128 mice are protected against the subtle Mn-induced behavioral changes and decreased striatal neuron density observed in Mn-exposed WT mice.

1. Introduction

Maintaining appropriate manganese (Mn) homeostasis is crucial because excessive accumulation of this essential micronutrient is toxic [1,2]. Mn is required as an enzymatic cofactor in biological processes such as amino acid synthesis, antioxidant defense, and cellular metabolism. Adequate Mn is acquired through dietary sources and deficiency is rare [3-5]. Overexposure and Mn-induced toxicity are more commonly studied given the detrimental impact this has on brain health [6]. Mn and other heavy metal imbalances have been implicated in several neurological diseases including Huntington disease (HD) and Alzheimer's disease (AD) [7,8].

Mn transport and regulation are complex biological processes that are not completely understood. Exposure route, age, sex, and certain genetic mutations influence Mn accumulation [6,9-11]. For example, mutations in *SLC30A10* decrease Mn efflux and thus result in hypermanganesemia and neurologic abnormalities [12,13]. A disease-toxicant interaction was first identified between HD and Mn in a mouse striatal cell line, in which HD cells were less sensitive to Mn-induced toxicity compared to control cells [14]. This resistance to Mn toxicity was replicated in the same striatal HD cells and human neuroprogenitors [15]. We have previously reported decreased responsiveness to global Mn-induced changes across several Mn exposure paradigms in HD mouse models during both pre-manifest and manifest disease stages [16]. These studies strongly suggest that HD can impact Mn homeostasis.

HD is a neurodegenerative disorder caused by an autosomal dominant mutation in the *Huntingtin (HTT)* gene. Clinical presentation includes psychiatric and cognitive impairments, but the most notable symptoms are chorea and associated motor deficits. Progressive cell death of the medium spiny neurons (MSNs) in the striatum (caudate and putamen) constitutes the hallmark neuropathology observed in HD [17,18]. Brain areas that accumulate the highest concentrations of Mn include HD phenotype-relevant areas such as basal ganglia (globus pallidus and substantia nigra) [19] and one outcome of excess Mn exposure is a Parkinsonian-like motor condition known as Manganism [20,21]. Decreased bioavailable Mn has been reported in cell and animal models of HD prior to disease onset [22] Activity of Mn-dependent enzymes arginase 2 (ARG2), Mn-superoxide dismutase

(MnSOD), and glutamine synthetase are also decreased in HD models and postmortem HD patient brains [23-25]. There are functional consequences to this decreased bioavailable Mn and lower enzymatic activity, evidenced by abnormalities in the urea cycle [26,27]. We have previously shown rescue of several HD phenotypes following Mn treatment. Impairments in the urea cycle, autophagic cargo load, and glucose uptake were attenuated by acute Mn exposure [22,28,29]. Not all HD phenotypes examined have been positively affected by Mn. HD-related differences in cholesterol metabolism were unaffected by Mn treatment [30]. Despite generally showing decreased responsiveness, the YAC128 mouse model of HD was shown to more sensitive to neurite damage by acute Mn exposure than controls when examining decreased dendritic complexity by Mn exposure in striatal MSNs [31].

In the present study we studied for the first time the HD-Mn interaction with a chronic Mn exposure paradigm in the YAC128 mouse model of HD. The YAC128 model is a full-length transgenic line that recapitulates key features of HD such as progressive motor impairments and selective striatal atrophy. Early deficits in motor learning have been reported at 2 months of age in these mice with impairments progressively worsening at 4-6 months and older [32-34]. In the current study, Mn treatment began at 12 weeks of age (3 months), prior to substantial behavioral deficits and striatal cell loss presenting in YAC128 mice. Mice were chronically exposed to $MnCl_2 \cdot 4(H_2O)$ via twice weekly subcutaneous injections for 20 – 40 weeks and underwent behavioral testing prior to measuring tissue Mn levels and Mn-induced protein changes in the striatum. We hypothesized that behavioral HD phenotypes would be ameliorated or prevented by chronic Mn exposure and HD mice would be protected against toxic effects experienced by wild-type (WT) mice from this long-term chronic Mn exposure.

2. Materials and Methods

2.1 Animals

FVB-Tg(YAC128)53Hay/J mice (Jackson Laboratory, Bar Harbor, ME; stock number: 027432) were originally obtained from Jackson Laboratories and used to found the mouse colony for these studies. These mice carry 3 copies of the *Huntingtin* gene – both wild-type (WT) copies of mouse *Huntingtin (Htt)* and one full-length copy of human mutant *Huntingtin* (*HTT)* – and will be referred to as YAC128. Hemizygous YAC128 males/females were bred with opposite sex WT mice from the same colony to maintain the line. Mice were weaned at 3 weeks old and housed in groups of 2-5; on occasion, mice were singly housed if cage mates became aggressive or died mid-study, which was not believed to be genotype or treatment related given comparable losses among groups (0-2 per genotype-treatment-sex group). Genotyping was performed at 3 weeks old using Transnetyx, as previously described [22]. YAC128 mice model HD by exhibiting behavioral impairments by 4-6 months which progressively worsen and that correlate to selective striatal neurodegeneration by 12 months old [32,34]. Approximately equal numbers of male and female mice were used in each genotype-treatment group. Mice had *ad libitum* access to standard lab chow (LabDiet 5L0D, TX) and water in a temperature- and humidity-controlled housing room on a 12:12 light:dark cycle. All protocols were approved by the Vanderbilt University Institutional

Animal Care and Use Committee under protocol number M1600073. All experiments were conducted in accordance with the NIH Guide for the Care and Use of Laboratory Animals.

2.2 Manganese exposures

Manganese chloride tetrahydrate ($MnCl_2 \cdot 4(H_2O)$, Fisher Scientific) was made up in DI water as a 1% stock solution, filtered through a 0.2 μm membrane, and administered as 50 mg/kg body weight. The 1% stock solution was further diluted with filtered DI water to 0.1-0.4% for the 5 – 20 mg/kg body weight doses; filtered DI water was used as vehicle. All doses were administered at a volume of 5 mL/kg injected subcutaneously in the left or right (alternating) inguinal area using an insulin syringe (27 G, ½ inch). A 50 mg/kg $MnCl_2 \cdot 4(H_2O)$ corresponds to a dose of 13.8 mg/kg Mn^{2+}.

The acute exposure (Fig. 1A) is a previously adapted exposure paradigm [35]. At 12 weeks of age, mice (n=6-8 per genotype-treatment group, approximately equal males and females) were injected on days 1, 4, and 7 prior to sacrifice and dissection on day 8 (24 hours after the final injection).

2.2.1 Study 1.—Mice were injected twice weekly (Mondays and Thursdays) with one of four Mn doses [0, 5, 15, and 50 mg/kg $MnCl_2 \cdot 4(H_2O)$] starting at 12 weeks of age until 32 weeks of age, with sacrifice and dissection approximately 24 hours after the final injection (Fig. 2A). Mn treatment was randomly assigned prior to behavioral testing. Molecular outcome measurements (striatal Mn and ARG2 protein) for 0 and 50 mg/kg $MnCl_2 \cdot 4(H_2O)$ treated mice only were previously reported as a subset of additional measurements not included in the present study (striatal metabolomics) [16]. Only molecular measurements from mice that completed the entirety of behavioral testing are included here. N=7-11 per genotype-treatment group with approximately equal number of males and females in each group.

2.2.2 Study 2.—Mice were injected twice weekly (Mondays and Thursdays) with either vehicle (0) or 5 mg/kg $MnCl_2 \cdot 4(H_2O)$ starting at 12 weeks of age. Assignment to either vehicle or Mn was pseudo-random. We re-assigned exposure group so that the rotarod performance at 11 weeks was equivalent between assigned exposure groups within a genotype. At 31 weeks of age, half of the mice crossed over to the other treatment group; this was randomly pre-determined. The treatment cross over design allowed for higher power in the behavioral assays up to 30 weeks of age and simultaneously allowing examination of molecular changes from three unique chronic Mn exposures. The abbreviation “0_5” indicates the group that received vehicle and then Mn, and “5_0” is the group that were changed from Mn to vehicle at 31 weeks. Injections continued until 52 weeks and mice were sacrificed and dissected approximately 24 hours after the final injection (Fig. 4A). During the behavioral battery, injections were administered after completion of a behavioral task to avoid assessing acute effects in both Studies 1 and 2. Prior to treatment cross over, n=26-29 per genotype-treatment group and after treatment cross over n=12-15 per genotype-treatment group with approximately equal number of males and females in each group.

2.3 Behavioral testing

2.3.1 Elevated zero maze (EZM).—A standard black elevated zero maze (EZM; San Diego Instruments, CA) was used to assess exploratory and anxiety-like behavior. A mouse was placed in an open zone and freely explored for 5 minutes. The task was recorded by a camera suspended from the ceiling above the maze and time spent in each zone was analyzed using AnyMaze (Stoelting Co., IL). An experimenter monitored the recording of the task live in an adjacent room.

2.3.2 Inverted screen.—A wire mesh screen (approximately 30 x 7.5 cm) was mounted horizontally on a metal rod and plexiglass dividers created four 7.5 x 7.5 cm compartments. A single mouse was placed in each of the four chambers. The rod was slowly rotated 90° and returned to its original position three times to ensure mice gripped the mesh screen with all four paws before rotating the rod a full 180° to an inverted position. The screen was 40 cm above the padded apparatus floor. Latency to fall during three trials was recorded and averaged, with a maximum trial length of 60 s and a 5-10 min inter-trial interval.

2.3.3 Wire hang.—Mice were individually placed by their front paws on a thin circular wire suspended 30 cm above a padded table. The latency to achieve a stable position (all four paws, or three paws and a tail) was recorded (60 s max per trial). If a mouse fell, a maximum latency of 60 s was assigned. Mice performed two trials with a 5–10 min inter-trial interval.

2.3.4 Grip strength.—Grip strength was measured using a force meter (San Diego Instruments, San Diego, CA). Mice were allowed to grab a square wire grid with the two front paws while being held by the tail. When the mouse had a firm grip on the grid, the experimenter gently pulled the mouse back in a horizontal plane until the grip was broken, and maximum force (N) was measured automatically by the apparatus. Each mouse was given three trials and average force per mouse was used for analysis.

2.3.5 Locomotor activity.—Spontaneous locomotor activity was measured automatically via the breaking of infrared beams over 30 minutes in the open field using standard sound-attenuating, light- and air-controlled locomotor activity chambers (27 x 27 x 20.5 cm, ENV-510; MED Associates, VT).

2.3.6 Balance beam.—Motor coordination was assessed by the ability to traverse a circular horizontal beam (2.5 cm diameter, 80 cm long, suspended 51.5 cm above a table) between two platforms. The beam connected a small (5 cm x 10 cm) uncovered starting platform and a covered ending platform (18 cm x 18 cm) containing home cage bedding to encourage retreat into the area. Mice were placed on the starting platform and a timer started when they stepped on to the beam with all four paws. The time to cross the beam (max 30 s) and the number of hind paw slips were recorded. If a mouse fell, it was placed back on the starting platform. Two trials were completed and the average time to cross the beam was reported and the total accumulated number of hind paw slips was used for analysis.

2.3.7 Rotarod.—Motor coordination was measured using a standard rotarod apparatus (Ugo Basile). The rod was 3 cm in diameter, suspended approximately 25 cm above a plastic lever on to which mice fell. There were five equal compartments (6 cm length of rod) divided by beige plexiglass. An accelerating protocol was used in which the rod began rotating at 4 rpm and ramped up to a max speed of 40 rpm by 5 min. The rod was rotating at 4 rpm when mice were placed on the apparatus and a timer was started, recording the latency to fall from the rod. Mice completed three trials per day, max 5 min per trial, with inter-trial intervals of 15 - 30 minutes. The daily average time to fall for each mouse was used in analysis of data.

2.3.8 Test order.—For Study 1, baseline behavior was completed at 11 weeks of age and final behavior at 30 weeks of age. A mid-study behavioral battery was completed at 22 weeks of age to confirm that the HD phenotype had not progressed so far as to reach a floor effect in any time at this age. Data were analyzed and group differences did not differ from baseline/final behavior and this is not reported for brevity of results. Testing order was Day 1: EZM and inverted screen, Day 2: locomotor activity and wire hang, Days 3-5: accelerating rotarod. In Study 2, baseline behavior was completed at 11 weeks of age. Mid-way study behavior was completed at 30 weeks of age and final behavior at 50 weeks of age. Behavioral batteries were also completed at 20 and 40 weeks to confirm HD-phenotypes had not progressed to a floor effect at these ages (not reported). Testing order was Day 1: EZM and inverted screen, Day 2: balance beam, Day 3: locomotor activity, Days 4-6: accelerating rotarod (only a single day of rotarod was completed for behavior after baseline testing). All behavioral testing was completed between 9am-1pm and each apparatus was cleaned with 10% ethanol between animals.

2.4 Tissue collection

2.4.1 Study 1 and acute Mn exposure.—Mice were sacrificed by cervical dislocation without anesthesia approximately 24 hours after the final injection. Mice were decapitated with sharp scissors and the brain removed from the skull. The brain was micro-dissected on ice under a dissecting microscope, collecting striatum and olfactory bulb. Liver tissue was also collected by cutting off a piece of the largest hepatic lobe. All tissue was flash frozen in liquid nitrogen and stored at −80° C until used for biochemical analyses.

2.4.2 Study 2.—Mice were euthanized approximately 24 hours following the final injection. Mice were deeply anesthetized using isoflurane and ~40-65 mL cold PBS (1.3x body weight) was perfused by pump. Mice were decapitated with sharp scissors, the brain (including olfactory bulbs and medulla) was removed, weighed (mg), and bisected with a razor blade. The left hemisphere immersion-fixed in 4% paraformaldehyde (PFA) for 8 days when hemispheres were then paraffin embedded and stored until all brains were collected and a tissue microarray was assembled. The right hemisphere was micro-dissected under a dissecting microscope on ice, collecting striatum and cortex. Liver was also collected. Fresh tissue was flash frozen in liquid nitrogen and stored at −80° C until later analysis (Mn levels and western blotting).

2.5 Tissue Mn levels

Mn concentrations were measured by graphite furnace atomic absorption spectroscopy (GFAAS, Varian AA240, Varian, Inc., Palo Alto, CA) using a protein lysate as previously reported [16].

2.6 Western blotting

Protein lysates were prepared by homogenizing frozen tissue by sonication in 100 – 400 μL Pierce RIPA lysis buffer (Thermo Scientific, cat # 89900) with protein and phosphatase inhibitors (Sigma Aldrich, cat # P0044, #P2850, #P5726, and #P2714) at 1:100 dilution. Lysates were spun down at 12,000 g for 10 min and supernatant collected. Protein concentration was measured using a standard bicinchoninic acid (BCA) assay protocol (Pierce BCA Protein Assay Kit, Thermo Scientific). Samples were prepared with 4x Laemmli sample buffer (Bio-Rad cat# 0610747) and 2-mercaptoethanol. For ARG2, samples were boiled for 5 min at 95° C and 40 μg protein was loaded onto 4–20% Criterion™ TGX™ Precast Midi Protein Gel (Bio-Rad cat #5671095). Gels were run at 90 volts for 120 min and transferred to nitrocellulose membranes using the iBlot™ system. Following transfer, gels were rehydrated in DI water overnight and stained with Coomassie (Bio-Rad, cat # 161-0786) for 60 min for use as a loading control. Membranes were blocked for 60 min in Odyssey Blocking Buffer (Odyssey cat # 927-40000) prior to blocking in primary anti-ARG2 at 1:1000 (Santa Cruz, sc-20151) overnight at 4° C. Membranes were washed with TBST prior to incubation for 120 min in anti-rabbit secondary (Licor IRDye 700 or 800CW) diluted 1:10,000 in Odyssey blocking buffer. Protein bands were detected using the Odyssey infrared system and analyzed with ImageStudio Lite (www.licor.com) and normalized to total protein quantified from Coomassie stained gel signal and then the average WT vehicle signal per blot. For GLT-1, samples were not boiled and 10 μg protein was loaded onto Bolt™ 4-12% Bis-Tris Plus gels (Thermo Scientific, cat # NW04120BOX) and run for 30 min at 200 volts prior to transfer on to nitrocellulose membranes (Thermo Scientific, cat # IB23001) using the iBlot2™ system. Gels were rehydrated in DI water overnight and Coomassie stained as described above. Membranes were blocked in 5% nonfat milk in TBST for 1 h prior to incubation overnight with primary anti-GLT-1 at 1:4,000 (Millipore Sigma, AB1783). Membranes were washed with TBST prior to incubation with HRP-conjugated anti-guinea pig secondary at 1:10,000 in 5% nonfat milk in TBST for 2 h. Protein bands were detected by chemiluminescence (Perkin Elmer, Western Lightning Plus-ECL, cat # NEL104001EA) and analyzed with ImageJ (imagej.nih.gov). For GLT-1, signal intensity was normalized to Coomassie stained gel signal and reported as arbitrary units. Glial fibrillary acidic protein (GFAP) at 1:5,000 (Millipore Sigma, G3893) and ionized calcium binding adaptor molecule 1 (Iba1) at 1:2,000 (FUJIFILM Wako Pure Chemical Corporation, 019-19741) were probed on a third set of blots performed using the same protocol described above for GLT-1 but 30 μg protein from a cortical lysate was loaded. HRP-conjugated anti-mouse and anti-rabbit secondary at 1:5,000 were used, respectively.

2.7 Immunohistochemistry

2.7.1 Tissue microarray.—To minimize technical variability and maximize the number of mice represented on a histological slide, a tissue microarray (TMA) was constructed by the VUMC Translational Pathology Shared Resource. Paraffin embedded hemispheres were sectioned coronally until visualization of the anterior commissure (+1.1 to +0.5 mm relative to bregma), a 4 μM thick section was H&E stained and used to annotate a 2 mm core encompassing the striatum. Embedded brain blocks were loaded on to the TMA Grandmaster (PerkinElmer) automated arrayer and the machine automatically constructs a TMA by removing cores from donor blocks based on annotations provided by the experimenter. Following construction, an H&E slide was made and evaluated for quality. From the TMA block (~50 cores/mice per block), 20 μM thick sections were cut and mounted for staining. Four TMA slides (200 microns apart) were stained with NeuN (below) for cell counting.

2.7.2 NeuN staining.—Slides were placed on a Leica Bond Max IHC Stainer. All steps except dehydration, clearing and cover slipping were performed on the Bond Max. Slides were deparaffinized. Heat induced antigen retrieval was performed on the Bond Max using Epitope Retrieval 1 solution for 20 minutes. Slides were incubated with anti-NeuN 1:2,500 (MAB377, Millipore Sigma) for 15 min. The Bond Polymer Refine detection system was used for visualization. Slides were dehydrated, cleared and cover slipped.

2.7.3 Striatal cell counts.—Each core was visualized at 4x magnification (EVOS Core XL) and evaluated for quality. Tissue cores that were damaged (i.e., folded over on itself or missing tissue) were excluded from analysis. Three non-overlapping 40x magnification images (850 μm by 650 μm area) were taken per core, per slide (total 12 images per mouse). Cell counting was performed using ImageJ automated software. In brief, 40x images were converted to 16-bit, threshold was adjusted to highlight cells visualized by NeuN staining, watershed algorithm applied and particles greater than 1200 square-pixels and with 0.35-1.00 circularity counted. These parameters were set based on first two independent experimenters manually counting cells in 10 images and optimizing the automated protocol to match manual counts. From each set of counts per mouse, to reduce the effect of individual outliers the three values that clustered together the most closely were averaged to give a final representative cell count used for comparisons between groups. NeuN, rather than the specific MSN marker DARPP-32, was used as a neuronal marker as it was predicted to have greater statistical power in detecting striatal cell density differences in YAC128 mice[32].

2.8 Statistics

Data are reported as mean ± S.E.M. unless otherwise noted. Data analyses were completed in SPSS 26.0 or GraphPad Prism 8. All analyses were first run with sex as a fixed variable. There were no meaningful differences according to sex, and thus all data were collapsed and analyzed together except for body weight data. For all dependent variables, two-way univariate ANOVA (2 genotype x 2-4 treatments) was conducted with appropriate post-hoc follow up tests. Repeated measures (RM)-ANOVA was used for rotarod at baseline. Non-parametric tests were used when appropriate and noted in the results section. Outliers were

removed if due to experimental error and if outside of 95% confidence interval. Results were considered statistically significant if $P < 0.05$.

3. Results

3.1 YAC128 mice were less sensitive to acute Mn exposure

A one-week 50 mg/kg $MnCl_2 \cdot 4(H_2O)$ injection paradigm has previously been reported to increase both Mn concentration [14,35] and arginase 2 (ARG2) protein levels in the striatum [16,22]. Twelve-week-old mice were injected subcutaneously with vehicle (0), 10, 20 or 50 mg/kg $MnCl_2 \cdot 4(H_2O)$ over one week to determine if lower concentrations would lead to the same ARG2 increase and to estimate an approximate EC_{50} for Mn-induced changes in ARG2 protein expression (Fig. 1A). Mn increased striatal ARG2 in both genotypes (Treatment $F_{3, 51}=19.07$, $P<0.0001$, Genotype $F_{1, 51}=2.867$, $P=0.096$). Both 20 and 50 mg/kg $MnCl_2 \cdot 4(H_2O)$ significantly increased ARG2 protein in WT but only the 50 mg/kg $MnCl_2 \cdot 4(H_2O)$ dose increased ARG2 protein in YAC128 mice (Fig. 1B). We imputed an approximate EC_{50} of 10 mg/kg for the increase in ARG2 by Mn in WT and >20 mg/kg in YAC128, thus the approximate average EC_{50} (15 mg/kg) was implemented as one of three doses in the first of our chronic exposure behavioral studies that followed along with higher (50 mg/kg) and lower (5 mg/kg) doses.

3.2 Study 1 – Behavior

Acute (1-week) Mn exposure has previously been shown to rescue defects in the urea cycle of YAC128 mice [22] We sought to determine whether a long-term exposure to either 5, 15, or 50 mg/kg $MnCl_2 \cdot 4(H_2O)$ could lessen the severity of disease-relevant behavioral phenotypes (e.g., rotarod performance) in YAC128 mice and if the reported blunted response to global changes by Mn exposure would offer YAC128 mice protection against Mn-induced behavioral impairments (Fig. 2A). Behavior was first evaluated at baseline (Fig. 2B-2D; S-Fig. 1A-C) and the effect of Mn was determined in each of the 8 genotype-treatment groups at 30 weeks of age (Fig. 2E-G; S-Fig. 1D-F), after 18 weeks exposure to Mn.

3.2.1 Young YAC128 mice displayed a rotarod performance deficit—At 11 weeks of age, both genotypes showed appropriate motor learning during the accelerated rotarod task (Fig. 2B), as indicated by increased latency to fall over consecutive training days but YAC128 mice fell from the rod sooner than WT on all three days of the task (Day $F_{2, 66}=21.79$, $P<0.0001$, Genotype $F_{1, 66}=18.90$, $P<0.0001$) suggesting a motor coordination deficit.

The additional tasks in the behavioral battery performed at 11 weeks of age established that a rotarod impairment already existed in the YAC128 mice prior to the start of Mn exposure, which was not due to differences in anxiety-like behavior, activity levels, strength, or weight (S-Fig. 1). Mn dose was assigned randomly to each mouse prior to any behavioral testing and started following the completion of baseline behavior at 12 weeks of age.

3.2.2 Chronic low-dose $MnCl_2 \cdot 4(H_2O)$ protected rotarod performance decline in YAC128 mice—Rotarod performance at 30 weeks was analyzed as a fold-

change compared to baseline to avoid the expected confound of genotype differences in the degree of age-related decline. WT performance on the rotarod remained relatively stable between 11- and 30-weeks of age (no fold-change) and YAC128 vehicle-treated mice declined to approximately 57% of their 11-week performance (Genotype $F_{1, 60}$= 1.249, P=0.268, Treatment $F_{3, 60}$= 0.788, P=0.505, Interaction $F_{3, 60}$=4.391, P=0.007). However, performance in YAC128 mice exposed to low-dose 5 mg/kg $MnCl_2$ • 4(H_2O) did not change, suggesting a protective effect against progressive rotarod decline (Fig. 2E).

3.2.3 Chronic high dose $MnCl_2$ • 4(H_2O) exposure led to modest behavioral changes in WT mice—

WT mice that received the highest dose (50 mg/kg) of $MnCl_2$ • 4(H_2O) showed subtle changes in behavior during the EZM and open field tasks at 30 weeks of age. There was no significant difference in time spent in the open zone of the EZM between genotypes, but a Mn effect approached significance (Genotype $F_{1, 60}$= 0.035, P=0.852, Treatment $F_{3, 60}$= 2.602, P=0.060). Given that YAC128 mice exhibit blunted responses to Mn, we examined the effect of Mn within WT only to ensure sensitivity to detect Mn-induced changes and found that the WT mice receiving 50 mg/kg $MnCl_2$ • 4(H_2O) spent significantly more time in the open zone compared to vehicle-treated WT mice (Fig. 2F). In the locomotor activity chambers the same group of high-dose Mn-exposed WT mice were significantly less active compared to WT vehicle mice (Genotype $F_{1, 59}$= 0.489, P=0.487, Treatment $F_{3, 59}$= 4.261, P=0.009) (Fig. 2G). Weight, inverted screen, and wire hang performance were unaffected by Mn (P>0.05) (S-Fig. 1D-F).

3.3 Study 1 – Molecular biology

3.3.1 Mn accumulation occurred at a lower dose in brain than in liver—

Mn injections led to significant accumulation in brain (striatum and olfactory bulb) and liver in both genotypes, but not at all doses (Fig. 3A). The 15 and 50 mg/kg $MnCl_2$ • 4(H_2O) doses increased Mn levels in striatum (Genotype $F_{1, 60}$= 0.072, P=0.790, Treatment $F_{3,60}$= 58.25, P<0.0001) and olfactory bulb (Genotype $F_{1, 60}$=0.629, P=0.431, Treatment $F_{3, 60}$= 36.12, P<0.0001). Mn levels were generally higher in liver compared to brain, but only the 50 mg/kg dose resulted in a significant increase compared to vehicle (Genotype $F_{1, 60}$=0.208, P=0.650, Treatment $F_{3, 60}$= 9.725, P<0.001).

3.3.2 Mn increased striatal ARG2 in a dose-dependent manner—

Mn increased ARG2 protein levels in the striatum dose-dependently in both genotypes (Genotype $F_{1, 60}$=0.043, P=0.836, Treatment $F_{3, 60}$=21.27, P<0.0001) (Fig. 3B). In WT only 50 mg/kg $MnCl_2$ • 4(H_2O) led to a significant increase but in YAC128 mice both the 15 mg/kg and 50 mg/kg doses increased ARG2 compared to vehicle-treated mice within genotype.

3.4 Study 2 – Behavior

We sought to replicate the findings from Study 1 in a longer exposure paradigm in Study 2 (Fig. 4A). We selected the lowest (5 mg/kg) dose of $MnCl_2$ • 4(H_2O) for Study 2 because it prevented progressive decline on the rotarod in YAC128 mice and importantly did not lead to statistically significant Mn accumulation in brain, which could exert neurotoxic effects when maintained for the 18-week exposure. Study 2 examined if chronic exposure to low-dose (5 mg/kg) $MnCl_2$ • 4(H_2O) could prevent rotarod performance decline in YAC128 mice

at 30-weeks-old (Fig. 4E-G) and up to 12 months of age (Fig. 5). Following the behavioral battery at 30 weeks, half of the mice (randomly predetermined) switched treatment groups. This allowed us to assess the effects of continuous Mn exposure (5 mg/kg all 40 weeks, "5") compared to beginning exposure later in life (vehicle until 31 weeks old, followed by Mn for remainder of study, "0_5"), removing exposure (Mn first, followed by vehicle, "5_0"), or vehicle only (all 40 weeks, "0"). Further, we hypothesized YAC128 mice would be protected from any detrimental behavioral effects of Mn over a chronic (40-week) exposure given blunted response to exposures[16].

3.4.1 Young YAC128 mice displayed a deficit in rotarod performance—The same accelerating rotarod protocol was used at 11 weeks in Studies 1 and 2. Replicating the results found in Study 1 (Fig. 2B), YAC128 mice in Study 2 fell off the rod sooner and thus exhibited impaired rotarod performance as early as 11 weeks of age compared to WT. (Fig. 4B). Both genotypes displayed acceptable motor learning, with improved performance across test days (Day $F_{2, 107}$ =85.64, P<0.0001, Genotype $F_{1, 107}$=27.35, P<0.0001, Interaction $F_{2, 107}$=4.909, P=0.008). Young YAC128 mice did not display impairments on the balance beam task (P>0.05) nor were there meaningful differences in control behaviors assessed (S-Fig. 2A-C).

3.4.2 Young YAC128 mice exhibited normal behavior in baseline control tasks—Similar to Study 1, there were no main effects of or statistical interactions with sex as a variable so for all behavior analyses the sexes were combined in Study 2. During the EZM task, YAC128 mice spent slightly less time (148 s) in the open zone of the maze compared to WT (164 s) at 11 weeks of age (t_{106}=2.602, P=0.011). This genotype effect was driven by a subgroup of 5 YAC128 mice that spent <100 s in the open zone (Fig. 4C). Spending approximately 50% time in the open zone is considered normal and does not indicate an anxiety-like phenotype [37,38] and thus we do not believe that these data reflect a true anxiety phenotype in the YAC128 mice. During 30 minutes in the open field chamber, there was an approximately 10% decrease in total distance travelled in YAC128 mice compared to WT mice at 11 weeks (t_{107}=2.371, P=0.020) (Fig. 4D). The range of distance travelled was comparable between WT (2237-6000 cm) and YAC128 (2244-5873 cm) and is unlikely to have influenced the outcome on additional behavioral tasks such as the rotarod.

3.4.3 No significant behavioral effects of 18 weeks low dose $MnCl_2 \cdot 4(H_2O)$ exposure—From 11 weeks to 30 weeks of age, the latency to fall from the accelerating rotarod decreased significantly in all genotype and treatment groups (Genotype $F_{1, 105}$=35.890, P<0.0001, Treatment $F_{1, 105}$= 0.090, P=0.765, Age $F_{1, 105}$= 108.017, P<0.0001, all interaction Ps > 0.05). YAC128 vehicle-treated mice fell from the rod on average after 82.2 ± 34.3 s and Mn-treated YAC128 mice fell after 93.6 ± 43.1 s. Overall YAC128 mice displayed a motor coordination deficit compared to WT, who fell on average after 137.2 ± 54.0 s and 132.2 ± 45.2 s for vehicle and Mn-treated groups, respectively (raw data not shown). The fold-change from 11 to 30 weeks, after 18 weeks exposure to Mn or vehicle, is shown for all groups in Fig. 4E. WT mice fell from the rod on average 25% sooner at 30 weeks compared to 11 weeks, and YAC128 mice fell 31% sooner at 30 weeks

compared to 11 weeks; the change in performance was not significantly different between genotypes or Mn exposure groups. YAC128 mice did not display a motor coordination deficit on the balance beam task at 30 weeks of age (P>0.05) (S-Fig. 2E).

At 30 weeks of age, chronic Mn exposure did not influence time spent in the open zone of the EZM (Genotype $F_{1, 105}$ =2.376, P=0.126, Treatment $F_{1, 105}$=1.777) (Fig. 4F). Total distance travelled during 30 minutes in the open field was lower for YAC128 mice than WT, but Mn had no effect after this length of exposure (Genotype $F_{1, 104}$ =20.54, P<0.0001, Treatment $F_{1, 104}$=0.018, P=0.893) (Fig. 4G).

3.4.4 By 50 weeks of age YAC128 mice exhibited performance impairments on rotarod and balance beam—

On the rotarod, YAC128 mice fell from the rod sooner than WT and overall, both genotype groups declined significantly with age from 11 weeks (Genotype $F_{1, 101}$ =53.327, P<0.001, Treatment $F_{3, 101}$=0.132, P=0.941, Age $F_{1, 101}$=122.794, P<0.001, all interaction Ps > 0.05). Again, we analyzed the change in performance by plotting the fold-change of 50-week performance compared to 11-week performance (Fig. 5A). WT mice declined 6-40% and YAC128 mice declined 43-63% by 50 weeks of age, with no effect of Mn (Genotype $F_{1, 101}$ =11.54, P=0.001, Treatment $F_{3, 101}$=1.178, P=0.322). By this age, YAC128 mice also had a detectable motor coordination deficit on the balance beam task but performance in either genotype was unaffected by Mn (P>0.05) (S-Fig. 3B). Weight, general limb strength, and two-paw grip strength were not changed by Mn exposure in either genotype (P>0.05) (S-Fig. 3A, C, D).

3.4.5 Chronic Mn exposure led to subtle behavioral changes in WT but not YAC128 mice at 50 weeks—

At 50 weeks of age, there was no significant difference between genotypes or the four Mn exposure groups on time (s) spent in the open zone of the EZM (Genotype $F_{1, 101}$ =2.235, P=0.138, Treatment $F_{1, 101}$=0.236, P=0.075) (Fig. 5B). We also examined effect of *any* Mn exposure (5, 0_5, and 5_0 groups combined) compared to none (vehicle only) in each genotype because a blunted response was expected in YAC128 mice. In WT mice, any Mn exposure led to significantly decreased time spent in the open zone of the EZM compared to WT mice that never received Mn (t_{52}=2.642, P=0.012) but in YAC128 mice there was no effect of any Mn exposure (t_{53}=0.706, P=0.483). Similarly, there was no main effect of Mn for total distance travelled in the open field (Genotype $F_{1, 100}$ =37.15, P<0.001, Treatment $F_{1, 100}$=1.105, P=0.351) (Fig. 5C). Despite this, we again compared any Mn exposure against no Mn exposure and found no significant difference in total distance travelled in WT or YAC128 mice based on any Mn exposure (WT t_{51}=1.483, P=0.144; YAC128 t_{53}=1.061, P=0.293). Overall, YAC128 mice covered less distance than WT in the open field.

3.5 Study 2 – Molecular biology

3.5.1 Striatal NeuN positive cell density was significantly decreased by chronic Mn exposure in WT only—

YAC128 brains weighed significantly less than WT brains with no effect of Mn (Genotype $F_{1, 100}$ =18.99, P<0.0001, Treatment $F_{3, 100}$=0.124, P=0.946) (Fig. 6A). There was a 10% decrease in number of NeuN positive cells counted in the striatum of vehicle treated YAC128 mice compared to WT vehicle (P=0.0341)

(Genotype $F_{1, 98}$ =0.0644, P=0.8002, Treatment $F_{3, 98}$=0.8446, P=0.4247, Interaction $F_{3, 98}$=3.633, P=0.0156) (Fig. 6B), consistent with previous reports [32] Notably, the number of NeuN positive cells was significantly decreased (~10-12%) in the WT Mn exposure groups compared to WT vehicle (P=0.052, 0.015, and 0.016 for "5", "0_5", and "5_0" groups, respectively) but there was no significant difference in NeuN positive cell counts between any Mn treatment groups in YAC128 (P> 0.05). Representative images are shown in Fig. 6B ii.

3.5.2 Significant increases in brain and hepatic Mn levels were reversible—

Brain Mn was increased by exposure similarly between the genotypes (Fig. 6C). Mice that received Mn in the weeks immediately preceding sacrifice had significantly increased Mn in striatum (Genotype $F_{1, 98}$= 2.021, P=0.158, Treatment $F_{3, 98}$= 19.17, P<0.0001) and cortex (Genotype $F_{1, 92}$=0.032, P=0.856, Treatment $F_{3, 92}$= 19.51, P<0.0001). In WT, striatal Mn levels increased 2.1-fold compared to vehicle and 1.8-fold in "5" and "0_5" Mn treatment groups, respectively. These increases were not significantly different from each other (P=0.95), suggesting steady state levels were achieved for both exposures. In brain, WT and YAC128 mice that started the study on Mn but then switched to vehicle at 31 weeks ("5_0") had Mn levels that did not significantly differ from vehicle-treated mice (1.1- and 1.2-fold, respectively). This indicates that the increase, at least from exposure accumulating from 12-31 weeks of age, was reversible in brain tissue. In the liver, Mn accumulation differed by genotype (Genotype $F_{1, 98}$=8.004, P=0.0057, Treatment $F_{3, 98}$= 11.38, P<0.0001). Mn was significantly higher in YAC128 mice than WT receiving 5 mg/ $MnCl_2 \cdot 4(H_2O)$ for the entirety of the study. Again, in both genotypes, hepatic Mn levels returned to normal (not significantly different from vehicle) in mice that switched from Mn to vehicle exposures at the 31-week mark.

3.5.3 Continuous chronic Mn exposure increased striatal ARG2 protein expression—

Striatal Mn-dependent ARG2 was increased by Mn exposure in both genotypes but this was only significant following exposure throughout the entirety of the study (Genotype $F_{1, 57}$= 0.0146, P=0.904, Treatment $F_{3, 57}$= 8.433, P<0.0001) (Fig. 6D). We also measured the Mn-responsive protein, GLT-1, in striatum and found no effect of Mn exposure but YAC128 mice had significantly lower overall GLT-1 expression compared to WT (Genotype $F_{1, 92}$= 7.238, P=0.0085, Treatment $F_{3, 92}$= 0.437, P=0.727) (S-Fig. 4A). These findings suggest ARG2 expression levels are a more sensitive biomarker of Mn exposure than GLT-1. Cortical glial fibrillary acidic protein (GFAP) and ionized calcium binding adaptor molecule 1 (Iba1) expression were measured by western blot to assess gliosis and a neuroinflammatory response to chronic Mn but neither protein was expressed differently according to genotype or treatment (P>0.05) (S-Fig. 4B, C).

4. Discussion

We demonstrated that YAC128 mice respond differently to Mn exposure than WT mice across several behavioral tasks and molecular outcome measures. Following an acute exposure (three SC injections over one week) at 12-weeks of age, YAC128 mice were less sensitive to Mn-induced increases in striatal ARG2 protein. Increased ARG2 levels were comparable between genotypes at a high dose [50 mg/kg $MnCl_2 \cdot 4(H_2O)$], but

significant increases from baseline were only seen at lower doses [20 mg/kg $MnCl_2$ • $4(H_2O)$] in WT mice. The EC_{50} we approximated from this dose-response experiment was 2-fold greater (>20 mg/kg) in YAC128 compared to WT (10 mg/kg). We have previously reported impaired Mn uptake in YAC128 mice following acute high-dose exposure [14,16]. The mechanism for this decreased uptake is unknown but it is important to note at 12 weeks of age YAC128 mice do not exhibit striatal cell loss and therefore is not due to fewer cells [32] Further, the decreased Mn uptake phenotype following the same acute exposure is no longer present in aged (32 weeks) YAC128 mice despite significantly blunted responses to Mn on the striatal metabolome [16]. A higher EC50 in YAC128 mice is therefore not due to simple defects in accumulation but rather Mn bioavailability [22]

Because acute Mn exposures were successful in rescuing certain molecular HD phenotypes [22,28,29], We hypothesized that YAC128 mice exposed chronically to Mn would have attenuated behavioral phenotypes compared to vehicle treated YAC128 mice. Prior to Mn exposure (11 weeks of age), YAC128 mice exhibited performance deficits on the accelerated rotarod but normal locomotor activity, strength, and anxiety-like behavior. Our baseline behavioral findings are consistent with previous reports [36,37] though some studies do not detect motor impairments until 4 months of age [32] In Study 1, we observed that chronic low dose Mn [5 mg/kg $MnCl_2$ • $4(H_2O)$] prevented rotarod performance decline in YAC128 mice but higher doses did not provide the same protection. Importantly, the low dose did not result in detection of a significant increase in brain or hepatic Mn levels after 20 weeks exposure and there were no adverse behavioral effects on YAC128 mice from any of the three Mn doses in Study 1. This suggested that YAC128 mice could benefit from Mn at a dose that did not lead to significant, and potentially damaging, accumulation.

In Study 2, we exposed mice to only the lowest Mn dose [5 mg/kg $MnCl_2$ • $4(H_2O)$] from Study 1, or vehicle. We failed to detect the same protective effect of Mn against performance decline on the rotarod in Study 2. Unexpectedly, WT mice declined to the same extent as YAC128 in Study 2 which may reflect the different rotarod training paradigms used. Mice were re-trained on the rotarod (2 days training prior to testing on day 3) at each subsequent behavioral battery after 11 weeks in Study 1. These training days did not significantly change the group average rotarod performance and therefore were omitted in Study 2 to decrease the testing burden on the mice and limit ceiling-effects due to overtraining. In another study, YAC128 mice that were trained on the rotarod at 2 months and tested at 12 months were significantly impaired but still able to perform the task, but YAC128 mice that were not previously trained were unable to perform the rotarod at 12 months [34]. Others have reported a defect in motor learning consolidation in YAC128 mice [38]. It is possible that the combination of additional training and Mn exposure was required to exert protective effects as seen in Study 1. Alternatively, there may have also been unintended and unknown Mn exposure based on differences in rodent housing. Mice in Study 1 were co-housed with mice in various Mn treatment groups, including the highest dose of 50 mg/kg $MnCl_2$ • $4(H_2O)$. Mn is excreted in the feces [39] and thus mice in Study 1 may have been exposed to an effectively larger dose than in Study 2 by inhalation of dust within the cage. The decreased Mn uptake phenotype in YAC128 mice is present following an acute exposure at 12 weeks [16,22] but this phenotype is not detectable in aged (42 weeks) female YAC128 mice [22], nor do we report genotype differences in brain Mn accumulation in our current study.

Therefore, it is possible that a “pre-loading” with higher doses of Mn could benefit YAC128 mice prior to the presentation of motor deficits. Similarly pre-treatment with copper via either intraperitoneal injection or drinking water was neuroprotective against the excitotoxic damage observed in the quinolic acid rat model of HD [40,41]. It remains unknown if the systemic subcutaneous Mn injections were able to impact brain Mn bioavailability. Thus, it remains untested if elevated bioavailable Mn in the brain could be therapeutic or protective in HD models.

We hypothesized that YAC128 mice would be resistant to Mn-induced impairments and thus have a greater lowest- or no-observed effect level (LOEL/NOEL) for Mn compared to WT. In Study 1, WT mice exposed to the highest Mn dose [50 mg/kg $MnCl_2 \cdot 4(H_2O)$] exhibited behavioral changes by spending more time in the open zone of the EZM and were overall less active in the open field but neither behavior was affected in YAC128 mice. Decreased locomotor activity in WT was an expected outcome of Mn-induced toxicity [42-45] though transient increases in locomotor activity have also been documented following Mn exposure [46,47]. Reported effects of Mn on exploratory behavior or time spent in the open zone of the EZM are inconsistent [10,48]. In fact, we found the opposite effect on EZM behavior in Study 2, in which WT mice exposed to any Mn spent less time in the open zone of the EZM, indicative of an anxiety-like phenotype, with no Mn-induced changes in YAC128.

Interestingly, we did not observe Mn-induced impairments on the rotarod in the current study, inconsistent with outcomes in other reported exposures. Young (8-10 weeks of age) wild type C57Bl6 received Mn via drinking water for 6 weeks and using the same accelerating rotarod protocol as our study, deficits were detected in Mn-exposed WT at 14-16 weeks of age, but only in males. The same group of mice took longer to traverse the balance beam in another motor coordination task [49]. After 5 weeks of Mn exposure via drinking water, total brain Mn levels were approximately 2-fold greater than non-exposed mice (which is comparable to the striatal Mn increase in Study 2). A 14.7% reduction in rotarod performance was detected but this was only significant when comparing Mn- and vehicle-exposed mice in a model of hereditary hemochromatosis, not wild-type [50]. *Slc39a14*$^{-/-}$ mice accumulate Mn in all extra-hepatic tissues and also exhibit significant impairments on the rotarod [51]. Rats exposed to 0, 1 or 5 mg/kg $MnCl_2 \cdot 4(H_2O)$ via intraperitoneal injection 15 times over the course of 150 days exhibited significant rotarod impairments at the 5 mg/kg $MnCl_2 \cdot 4(H_2O)$ dose, but not the 1 mg/kg $MnCl_2 \cdot 4(H_2O)$[52] However, 5 mg/kg $MnCl_2 \cdot 4(H_2O)$ in rats is an effectively larger dose (~2 x) than in mice due to differences in metabolic rate [53]. Rodents in the aforementioned studies reporting effects were younger than in our study or required additional combined genetic factors to induce rotarod impairments following Mn exposure. Although rotarod performance was not significantly impaired, chronic Mn exposure resulted in a significant (10-12%) decrease in striatal NeuN positive cell density in WT. While NeuN is not a specific marker for MSNs, approximately 97% of neurons in the dorsal striatum are DARPP-32 positive MSNs [54], thus our reported findings likely affect this cell population. Others have reported Mn-induced cell loss in the globus pallidus [55], ventral tegmental area and substantia nigra pars compacta [42], but we focused on the striatum given its relevance to HD. YAC128 mice exhibited the expected 10% decrease in striatal NeuN positive cell density [32] but were resistant to further Mn-induced changes. This suggests that despite concurrent HD-related neurodegenerative

processes in the striatum, the HD genotype protected the striatal neurons from chronic Mn-induced decreases in neuron density. This argues in favor of a hypothesis that the mechanism of striatal cell death in HD is distinct from the neurotoxic mechanisms of Mn-induced cytotoxicity in the striatum.

The current study was unique in terms of exposure length and route – to our knowledge it is the longest reported Mn exposure by subcutaneous injection, which bypasses the gut and first-pass hepatic metabolism [39,56]. The subtle changes observed in specific outcome measures (behavior in the elevated zero maze, decreased striatal NeuN positive cell density, and increased striatal ARG2 levels), but not others (e.g., rotarod and balance beam performance), following long-term low-level Mn exposure in WT mice delineate the neurobehavioral and neuropathological effects at the threshold of chronic Mn toxicity. Interestingly, these most sensitive outcome measures are not directly related to motor function, rather our data suggest anxiety-like or exploratory behaviors, as well as Mn-dependent enzyme and neuronal density as the most sensitive measures of Mn neurotoxicity in long-term low-dose exposures. Other studies of appreciable length have employed different exposure routes, such as diet, drinking water, and inhalation [11,57-59] or include case-studies of exposure via total parenteral nutrition [60]. Exposure route, length, and chemical species are all critical determinants of toxicity outcomes outlined in a comprehensive review[61]. Our study is also unique in its randomized crossover design, with some animals receiving Mn in the earlier part of the study but not in the weeks immediately preceding sacrifice. We found that tissue Mn levels in those mice returned to levels that matched untreated mice, suggesting that if excess Mn exposure is terminated then levels can decrease to normal. However, significant behavioral impairments likely extend beyond normalized tissue levels of Mn, evidenced by mice receiving any Mn showing subtle deficits in the current study and by significant striatal cell loss in all Mn treated WT mice. A 1999 cross-sectional study examined the reversibility of neurobehavioral markers of chronic (8 year) excess Mn inhalation exposure in battery plant factory workers following mitigation of exposure and found that impairments were mostly irreversible [62].

Conclusions

This study contributes to our knowledge of Mn toxicity and homeostasis by providing additional evidence of an HD-Mn interaction, such that YAC128 mice are less sensitive to Mn exposure than WT. Future studies are needed to confirm whether alternate dosing paradigms can more consistently protect against declining motor function, and to elucidate the mechanism underlying this protection so that it may be exploited for potential new therapeutic approaches.

Supplementary Material

Refer to Web version on PubMed Central for supplementary material.

Acknowledgements:

We would like to thank Dr. John Allison for assistance with the design and execution of behavioral testing, which was performed in the Vanderbilt Mouse Neurobehavioral laboratory which receives support from the Vanderbilt Kennedy Center (P50 HD103537). We acknowledge the Vanderbilt University Medical Center (VUMC)

Translational Pathology Shared Resource (TPSR) supported by NCI/NIH Cancer Center Support Grant 5P30 CA68485-19 and the Shared Instrumentation Grant S10 OD023475-01A1 for the Leica Bond RX.

Funding:

This work was supported by NIH R01 ES016931 (ABB) and NIH R01 ES031401 (ABB and FEH). JMW and ACP were supported by T32 ES007028. JMW was supported by T32 AG058524.

References

1. Pfalzer AC & Bowman AB Relationships Between Essential Manganese Biology and Manganese Toxicity in Neurological Disease. Curr. Environ. Heal. reports 4, 223–228 (2017).
2. Horning KJ, Caito SW, Tipps KG, Bowman AB & Aschner M Manganese Is Essential for Neuronal Health. Annu. Rev. Nutr 35, 71–108 (2015). [PubMed: 25974698]
3. Aschner JL & Aschner M Nutritional aspects of manganese homeostasis. Mol. Aspects Med 26, 353–362 (2005). [PubMed: 16099026]
4. Aschner M Manganese Homeostasis in the CNS. Environ. Res 80, 105–109 (1999). [PubMed: 10092401]
5. Balachandran RC et al. Brain manganese and the balance between essential roles and neurotoxicity. J. Biol. Chem 295, 6312–6329 (2020). [PubMed: 32188696]
6. O'Neal SL & Zheng W Manganese Toxicity Upon Overexposure: a Decade in Review. Curr. Environ. Heal. reports 2, 315–328 (2015).
7. Bowman AB, Kwakye GF, Herrero Hernández E & Aschner M Role of manganese in neurodegenerative diseases. J. Trace Elem. Med. Biol 25, 191–203 (2011). [PubMed: 21963226]
8. Mezzaroba L, Alfieri DF, Colado Simão AN & Vissoci Reiche EM The role of zinc, copper, manganese and iron in neurodegenerative diseases. Neurotoxicology 74, 230–241 (2019). [PubMed: 31377220]
9. Chen P, Parmalee N & Aschner M Genetic factors and manganese-induced neurotoxicity. Front. Genet 5, 265 (2014). [PubMed: 25136353]
10. Moreno JA et al. Age-dependent susceptibility to manganese-induced neurological dysfunction. Toxicol. Sci 112, 394–404 (2009). [PubMed: 19812362]
11. Erikson KM, Dorman DC, Lash LH, Dobson AW & Aschner M Airborne manganese exposure differentially affects end points of oxidative stress in an age- and sex-dependent manner. Biol Trace Elem Res 100, 49–62 (2004). [PubMed: 15258319]
12. Mukhopadhyay S Familial manganese-induced neurotoxicity due to mutations in SLC30A10 or SLC39A14. Neurotoxicology 64, 278–283 (2018). [PubMed: 28789954]
13. Chen P, Bowman AB, Mukhopadhyay S & Aschner M SLC30A10: A novel manganese transporter. Worm 3, (2015).
14. Williams BB et al. Disease-toxicant screen reveals a neuroprotective interaction between Huntington's disease and manganese exposure. J. Neurochem 112, 227–237 (2010). [PubMed: 19845833]
15. Tidball AM et al. A novel manganese-dependent ATM-p53 signaling pathway is selectively impaired in patient-based neuroprogenitor and murine striatal models of Huntington's disease. Hum. Mol. Genet 24, 1929–1944 (2014). [PubMed: 25489053]
16. Pfalzer AC et al. Huntington's disease genotype suppresses global manganese-responsive processes in pre-manifest and manifest YAC128 mice. Metallomics 12, 1118–1130(2020). [PubMed: 32421118]
17. Finkbeiner S Huntington's disease. Cold Spring Harb. Perspect. Biol 3, 1–24 (2011).
18. Bates GP et al. Huntington disease. Nat. Rev. Dis. Prim 1, 1–21 (2015).
19. Yamada M et al. Chronic manganese poisoning: A neuropathological study with determination of manganese distribution in the brain. Acta Neuropathol. 70, 273–278 (1986). [PubMed: 3766127]
20. Hine CH & Pasi A Manganese Intoxication. West. J. Med 123, 101–107 (1975). [PubMed: 1179714]

21. Dobson AW, Erikson KM & Aschner M Manganese neurotoxicity. Handb. Neurotox 2, 843–864 (2014).
22. Bichell TJV et al. Reduced bioavailable manganese causes striatal urea cycle pathology in Huntington's disease mouse model. Biochim. Biophys. Acta - Mol. Basis Dis (2017). doi:10.1016/j.bbadis.2017.02.013
23. Butterworth J Changes in Nine Enzyme Markers for Neurons, Glia, and Endothelial Cells in Agonal State and Huntington's Disease Caudate Nucleus. J. Neurochem 47, 583–587 (1986). [PubMed: 2874190]
24. Carter CJ Glutamine synthetase activity in Huntington's Disease. Life Sci. 31, 1151–1159 (1982). [PubMed: 6128649]
25. Santamaría A et al. Comparative analysis of superoxide dismutase activity between acute pharmacological models and a transgenic mouse model of Huntington's disease. Neurochem. Res 26, 419–424 (2001). [PubMed: 11495354]
26. Patassini S et al. Identification of elevated urea as a severe, ubiquitous metabolic defect in the brain of patients with Huntington's disease. Biochem. Biophys. Res. Commun 468, 161–166 (2015). [PubMed: 26522227]
27. Handley RR et al. Brain urea increase is an early Huntington's disease pathogenic event observed in a prodromal transgenic sheep model and HD cases. Proc. Natl. Acad. Sci 114, E11293–E11302 (2017). [PubMed: 29229845]
28. Bryan MR et al. Acute manganese treatment restores defective autophagic cargo loading in Huntington's disease cell lines. Hum. Mol. Genet 28, 3825–3841 (2019). [PubMed: 31600787]
29. Bryan MR et al. Manganese Acts upon Insulin/IGF Receptors to Phosphorylate AKT and Increase Glucose Uptake in Huntington's Disease Cells. Mol. Neurobiol 57, 1570–1593 (2020). [PubMed: 31797328]
30. Pfalzer AC, Wages PA, Porter NA & Bowman AB Striatal Cholesterol Precursors Are Altered with Age in Female Huntington's Disease Model Mice. J. Huntingtons. Dis 8, 161–169 (2019). [PubMed: 30958310]
31. Madison JL, Wegrzynowicz M, Aschner M & Bowman AB Disease-toxicant interactions in manganese exposed Huntington disease mice: Early changes in striatal neuron morphology and dopamine metabolism. PLoS One (2012). doi:10.1371/journal.pone.0031024
32. Slow EJ et al. Selective striatal neuronal loss in a YAC128 mouse model of Huntington disease. Hum. Mol. Genet 12, 1555–1567 (2003). [PubMed: 12812983]
33. Van Raamsdonk JM, Warby SC & Hayden MR Selective degeneration in YAC mouse models of Huntington disease. Brain Res. Bull 72, 124–131 (2007). [PubMed: 17352936]
34. Van Raamsdonk JM Cognitive Dysfunction Precedes Neuropathology and Motor Abnormalities in the YAC128 Mouse Model of Huntington's Disease. J. Neurosci 25, 4169–4180 (2005). [PubMed: 15843620]
35. Dodd CA, Ward DL & Klein BG Basal ganglia accumulation and motor assessment following manganese chloride exposure in the C57BL/6 mouse. Int. J. Toxicol 24, 389–397 (2005). [PubMed: 16393931]
36. Kordasiewicz HB et al. Sustained Therapeutic Reversal of Huntington's Disease by Transient Repression of Huntingtin Synthesis. Neuron 74, 1031–1044 (2012). [PubMed: 22726834]
37. Garcia-Miralles M et al. Early pridopidine treatment improves behavioral and transcriptional deficits in YAC128 Huntington disease mice. JCI Insight 2, 1–18 (2017).
38. Glangetas C, Espinosa P & Bellone C Deficit in motor skill learning-dependent synaptic plasticity at motor cortex to Dorso Lateral Striatum synapses in a mouse model of Huntington's disease. eNeuro 7, 1–14 (2020).
39. Chen P, Bornhorst J & Aschner M Manganese metabolism in humans. Front. Biosci 23, 1655–1679 (2018).
40. Santamaría A et al. Copper blocks quinolinic acid neurotoxicity in rats: Contribution of antioxidant systems. Free Radic. Biol. Med 35, 418–427 (2003). [PubMed: 12899943]
41. Martínez-Lazcano JC et al. Sub-Chronic Copper Pretreatment Reduces Oxidative Damage in an Experimental Huntington's Disease Model. Biol. Trace Elem. Res 162, 211–218 (2014). [PubMed: 25319005]

42. Bouabid S, Delaville C, De Deurwaerdère P, Lakhdar-Ghazal N & Benazzouz A Manganese-induced atypical parkinsonism is associated with altered basal ganglia activity and changes in tissue levels of monoamines in the rat. PLoS One 9, (2014).
43. Cordova FM et al. In vivo manganese exposure modulates Erk, Akt and Darpp-32 in the striatum of developing rats, and impairs their motor function. PLoS One 7, (2012).
44. Vezér T et al. Behavioral and neurotoxicological effects of subchronic manganese exposure in rats. Environ. Toxicol. Pharmacol 19, 797–810 (2005). [PubMed: 21783557]
45. Asser A et al. Acute effects of methcathinone and manganese in mice: A dose response study. Heliyon 5, e02475 (2019). [PubMed: 31687570]
46. Nachtman JP, Tubben RE & Commissaris RL Behavioral effects of chronic manganese administration in rats: locomotor activity studies. Neurobehav. Toxicol. Teratol 8, 711–715 (1986). [PubMed: 3808186]
47. Avila-Costa MR et al. Manganese Inhalation Induces Dopaminergic Cell Loss: Relevance to Parkinson's Disease. Dopamine - Heal. Dis (2018). doi: 10.5772/intechopen.79473
48. Ye Q & Kim J Effect of olfactory manganese exposure on anxiety-related behavior in a mouse model of iron overload hemochromatosis. Environ. Toxicol. Pharmacol 40, 333–341 (2015). [PubMed: 26189056]
49. Freeman DM, O'Neal R, Zhang Q, Bouwer EJ & Wang Z Manganese-induced Parkinsonism in mice is reduced using a novel contaminated water sediment exposure model. Environ. Toxicol. Pharmacol 78, 103399 (2020). [PubMed: 32380377]
50. Alsulimani HH, Ye Q & Kim J Effect of Hfe deficiency on memory capacity and motor coordination after manganese exposure by drinking water in mice. Toxicol. Res 31, 347–354 (2015). [PubMed: 26877837]
51. Jenkitkasemwong S et al. SLC39A14 deficiency alters manganese homeostasis and excretion resulting in brain manganese accumulation and motor deficits in mice. Proc. Natl. Acad. Sci 115, E4730 (2018). [PubMed: 29735648]
52. Fan XM et al. Chronic Manganese Administration with Longer Intervals Between Injections Produced Neurotoxicity and Hepatotoxicity in Rats. Neurochem. Res 45, 1941–1952 (2020). [PubMed: 32488470]
53. Nair A & Jacob S A simple practice guide for dose conversion between animals and human. J. Basic Clin. Pharm 7, 27 (2016). [PubMed: 27057123]
54. Matamales M et al. Striatal medium-sized spiny neurons: Identification by nuclear staining and study of neuronal subpopulations in BAC transgenic mice. PLoS One 4, (2009).
55. Tapin D, Kennedy G, Lambert J & Zayed J Bioaccumulation and locomotor effects of manganese sulfate in Sprague-Dawley rats following subchronic (90 days) inhalation exposure. Toxicol. Appl. Pharmacol 211, 166–174 (2006). [PubMed: 16112697]
56. Davis CD, Zech L & Greger JL Manganese Metabolism in Rats: An Improved Methodology for Assessing Gut Endogenous Losses. Proc. Soc. Exp. Biol. Med 202, 103–108 (1993). [PubMed: 8424090]
57. Avila-Costa MR et al. Manganese inhalation as a Parkinson disease model. Parkinsons. Dis 2011, 1–14 (2011).
58. Komura J & Sakamoto M Effects of manganese forms on biogenic amines in the brain and behavioral alterations in the mouse: Long-term oral administration of several manganese compounds. Environ. Res 57, 34–44 (1992). [PubMed: 1740094]
59. Morganti JB, Lown BA, Stineman CH, D'Agostino RB & Massaro EJ Uptake, distribution and behavioral effects of inhalation exposure to manganese (MnO2) in the adult mouse. Neurotoxicology 6, 1–15 (1985).
60. Khan A, Hingre J & Dhamoon AS Manganese Neurotoxicity as a Complication of Chronic Total Parenteral Nutrition. Case Rep. Neurol. Med 2020, 1–6 (2020).
61. Gwiazda R, Lucchini R & Smith D Adequacy and consistency of animal studies to evaluate the neurotoxicity of chronic low-level manganese exposure in humans. J. Toxicol. Environ. Heal. - Part A Curr. Issues 70, 594–605 (2007).

62. Roels HA, Ortega Eslava MI, Ceulemans E, Robert A & Lison D Prospective study on the reversibility of neurobehavioral effects in workers exposed to manganese dioxide. Neurotoxicology 20, 255–271 (1999). [PubMed: 10385889]

Highlights

- Striatal neuron density was decreased 10-12% by chronic Mn in WT mice
- Decreased activity following chronic Mn exposure occurred in WT but not YAC128 mice
- Behavior in the elevated zero maze was altered by chronic Mn in WT only
- Mn-induced rotarod impairments were not observed in either genotype
- Brain [Mn] and ARG2 protein levels were increased by chronic Mn in both genotypes

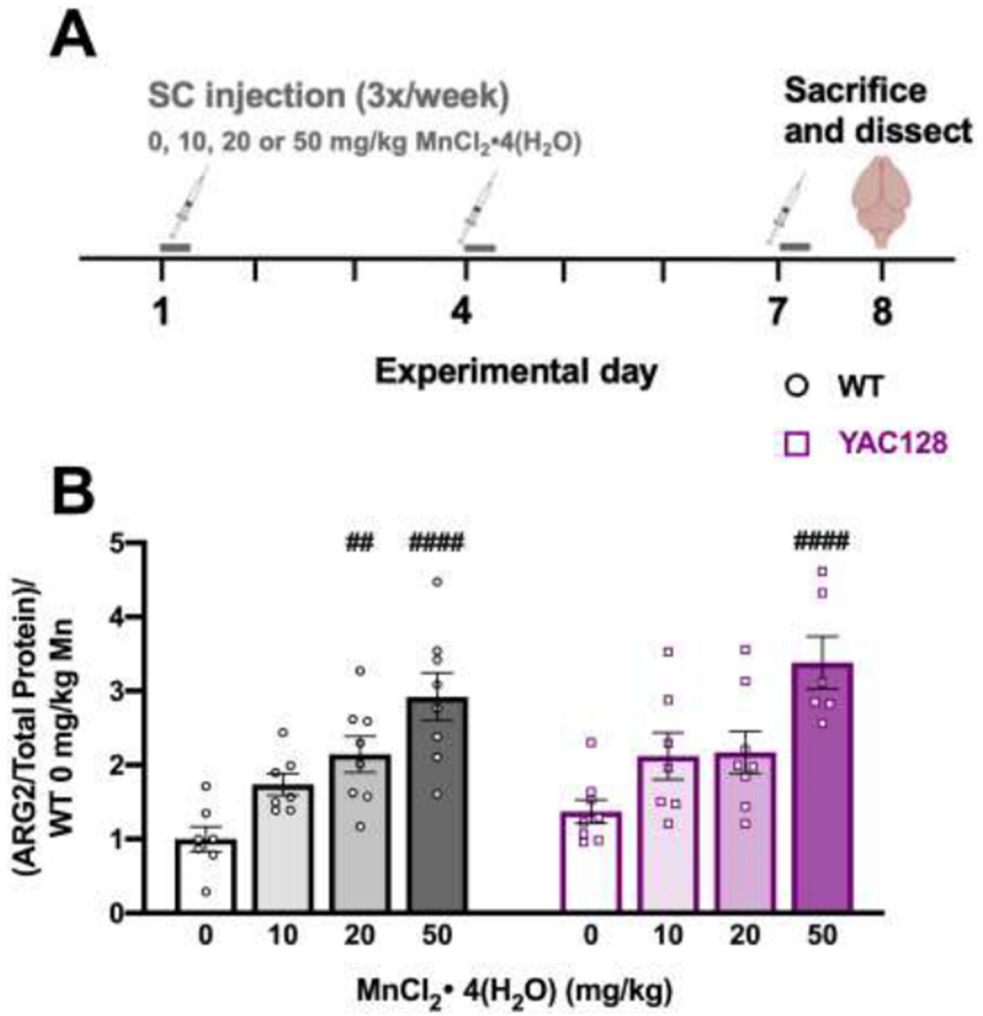

Figure 1.

Acute Mn exposure study. (**A)** Experimental timeline. At 12 weeks of age, mice were injected [0, 10, 20, or 50 mg/kg $MnCl_2$ • 4(H_2O)] 3 times over the course of one week (days 1, 4, and 7) and sacrificed 24 hours following the third injection (day 8). **(B)** ARG2 protein expression increased following Mn exposure in both genotypes but a larger dose is required in YAC128 mice compared to WT. Pound symbol indicates significant difference from vehicle within a genotype by post-hoc Dunnett's multiple comparisons. Mean ± S.E.M. plotted. ## $p<0.01$, ####$p<0.0001$. n=6-8 per genotype-treatment group, approximately equal males and females.

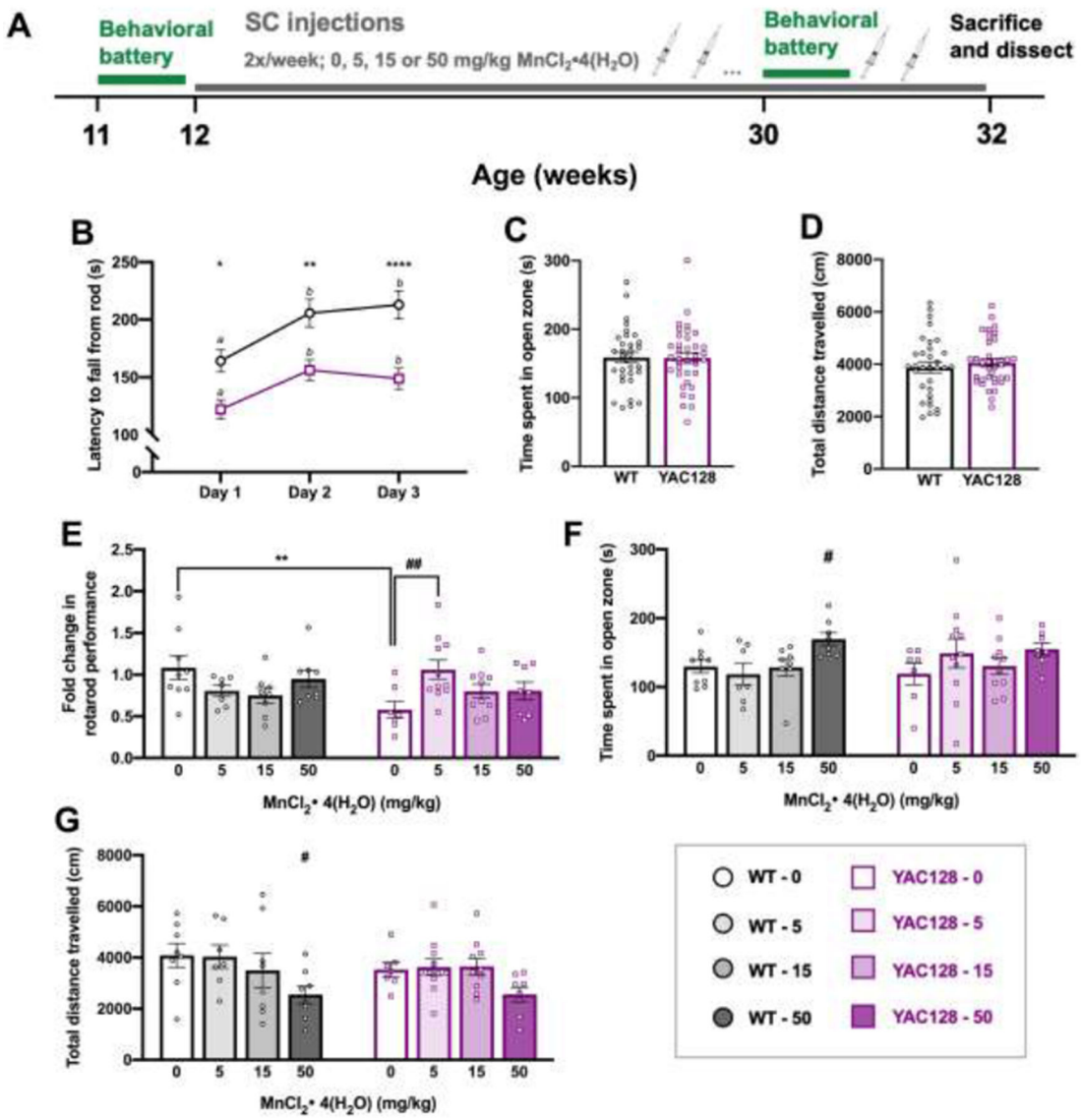

Figure 2.

Behavior chronic Study 1. **(A)** Experimental timeline for study 1 (n=68). Mice underwent a week-long baseline behavioral battery at 11 weeks old (B-D) prior to beginning twice weekly subcutaneous injections (0, 5, 15, or 50 mg/kg $MnCl_2 \cdot 4(H_2O)$) from 12 weeks until 32 weeks of age. The behavioral battery was repeated at 30 weeks of age (E-G) to assess effects of chronic Mn exposure and mice were sacrificed and dissected at 32 weeks of age, 24 hours after the final injection. **(B)** Average latency to fall (3 trials per day; 300 s max per trial) from the rotarod across 3 days. Both genotypes display appropriate motor learning during the task, indicated by increased latency to fall on days 2 and 3 compared to day 1. YAC128 mice fall from the rod sooner than WT on all three days. Asterisks indicate a significant difference between genotypes on that day, and days that do not share a superscript letter are significantly different from each other within a genotype. **(C)** Anxiety-like behavior during a novel behavioral task was similar between genotypes at 11 weeks of age measured by time (s) spent in the open zone of the elevated zero

maze (EZM). **(D)** Total distance travelled during 30 minutes in an open field chamber was comparable between WT and YAC128 mice. **(E)** Fold change in rotarod performance. Performance at 30 weeks for each individual mouse was divided by 11-week performance and plotted. Post-hoc follow-up tests showed that there was only a genotype difference in the vehicle dose (**), and within a genotype, the only significant Mn effect was between YAC128 vehicle and 5 mg/kg-exposed groups (##). **(F)** High dose Mn resulted in more time spent in the open zone of the EZM in WT mice. **(G)** WT mice receiving the highest dose of Mn were less active than vehicle-treated WT mice. For all, mean ± S.E.M. plotted unless otherwise noted. Asterisks * indicate genotype effect, pound # indicates Mn effect within genotype. # p <0.05, ## p <0.01, * p<0.05 **p<0.01, **** p<0.0001. n=7-11 per genotype-treatment group with approximately equal number of males and females.

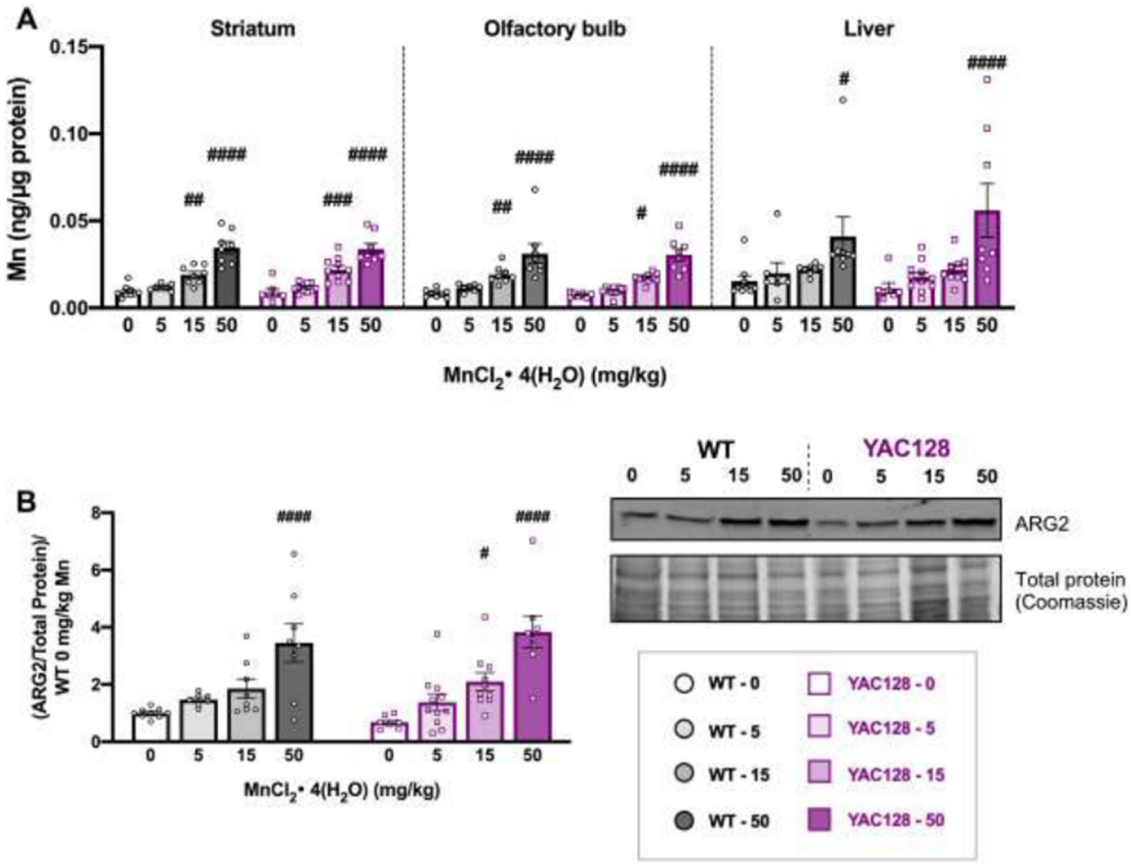

Figure 3.

Post-dissection outcomes for mice used in Study 1. (A) Mn levels (ng/µg protein) at 32 weeks of age for striatum (left), olfactory bulb (middle) and liver (right) from mice in Study 1 after 20 weeks of subcutaneous injections. Mn increased in all tissue types following exposure. Only 15 and 50 mg/kg significantly increased brain levels and only 50 mg/kg significantly increased hepatic Mn; # indicates significant differences from vehicle within each genotype by post-hoc Sidak's multiple comparisons. (B) ARG2 protein expression normalized to total protein on gels by Coomassie blue staining for loading control and normalized to average WT 0 for each blot. Mn increased ARG2 expression in both genotypes, which were not different from each other. Within a genotype, only the 50 mg/kg dose was significantly higher than vehicle in WT and both 15 and 50 mg/kg doses led to a significant increase compared to its own genotype vehicle in YAC128, indicated by #. Representative blot and Coomassie stained gel are shown. For all, mean ± S.E.M. plotted unless otherwise noted. # $p < 0.05$, ##, $p < 0.01$, ### $p < 0.001$, #### $p < 0.0001$. n=7-11 per genotype-treatment group with approximately equal number of males and females.

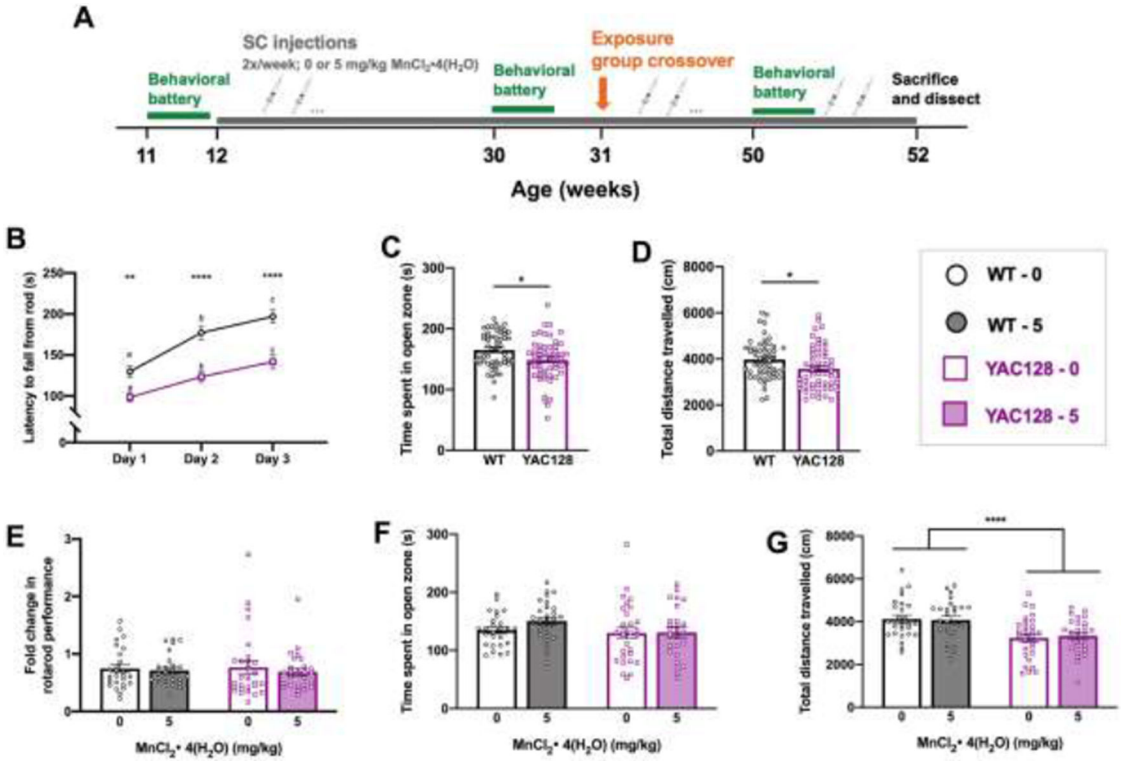

Figure 4.

Study 2 behavior up to 30 weeks of age. **(A)** Experimental timeline for Study 2. Mice underwent a week-long baseline behavioral battery at 11 weeks old (**B-D**) prior to beginning twice weekly subcutaneous injections [0 or 5 mg/kg $MnCl_2 \cdot 4(H_2O)$] at 12 weeks of age. The behavioral battery was repeated at 30 weeks of age **(E-G),** then half of the mice changed exposure groups at 31 weeks of age and behavioral battery was repeated at 50 weeks of age (see Fig. 5) prior to sacrifice and dissection (see Fig. 3.6) at 52 weeks of age. **(B)** Average latency to fall (3 trials per day; 300 s max per trial) from the rotarod across 3 days. Both genotypes displayed appropriate motor learning during the task, indicated by increased latency to fall on days 2 and 3 compared to day 1. YAC128 mice fall from the rod sooner than WT on all three days. Asterisks indicate a significant difference between genotypes on that day, and days that do not share a superscript letter are significantly different from each other within a genotype. **(C)** YAC128 mice spent less time in the open zone of the EZM compared to WT at 11 weeks of age, however this was driven by the 5 YAC128 mice that spent <100 s in the open zone and does not indicate anxiety-like behavior in either group. **(D)** YAC128 mice on average covered less distance than WT in 30 minutes of the open field, however the range of distance travelled is similar between genotypes. **(E)** Fold change in rotarod performance at baseline (11 weeks) to the 30-week assessment. Performance of each individual mouse at 30 weeks was divided by 11-week performance. On average there was a 25% decrease in performance for WT mice and 31% decrease for YAC128 mice. **(F)** There was no difference between genotypes or treatment groups for time spent in open zone of the EZM at 30 weeks. **(G)** Total distance travelled during 30 minutes in the open field. YAC128 mice travelled less than WT, but there was no effect of Mn after this length of exposure. For all, mean ± S.E.M. plotted unless otherwise noted. Asterisks *

indicate genotype effect. * p <0.05, **, p<0.01, *** p<0.001, **** p<0.0001. n=26-29 per genotype-treatment group with approximately equal number of males and females.

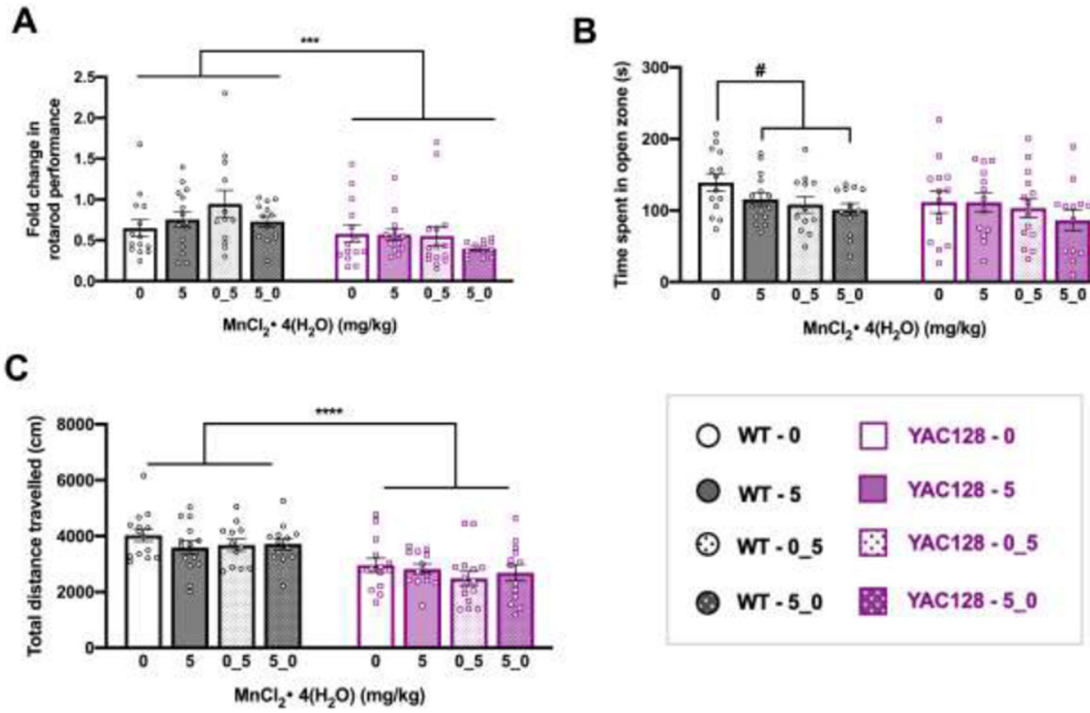

Figure 5.

Behavior for mice from Study 2, at 50 weeks (experimental timeline shown in Figure 4A). **(A)** Fold change in rotarod performance from 11 to 50 weeks of age. On average, all groups performed worse on the task at 50 weeks compared to 11 weeks. YAC128 mice performance declined to a greater extent than WT. **(B)** Time spent in open zone of the EZM at 50 weeks. The three WT groups that received any Mn exposure combined were significantly different from vehicle treated WT mice by t-test. **(C)** Total distance travelled during 30 minutes in the open field. YAC128 mice travelled less than WT, with no effects of any length Mn exposure in either genotype. For all, mean ± S.E.M. plotted unless otherwise noted. Asterisks * indicate genotype effect, pound # indicates Mn effect within genotype. #/* p <0.05, **, p<0.01, *** p<0.001, **** p<0.0001. n=12-15 per genotype-treatment group with approximately equal number of males and females.

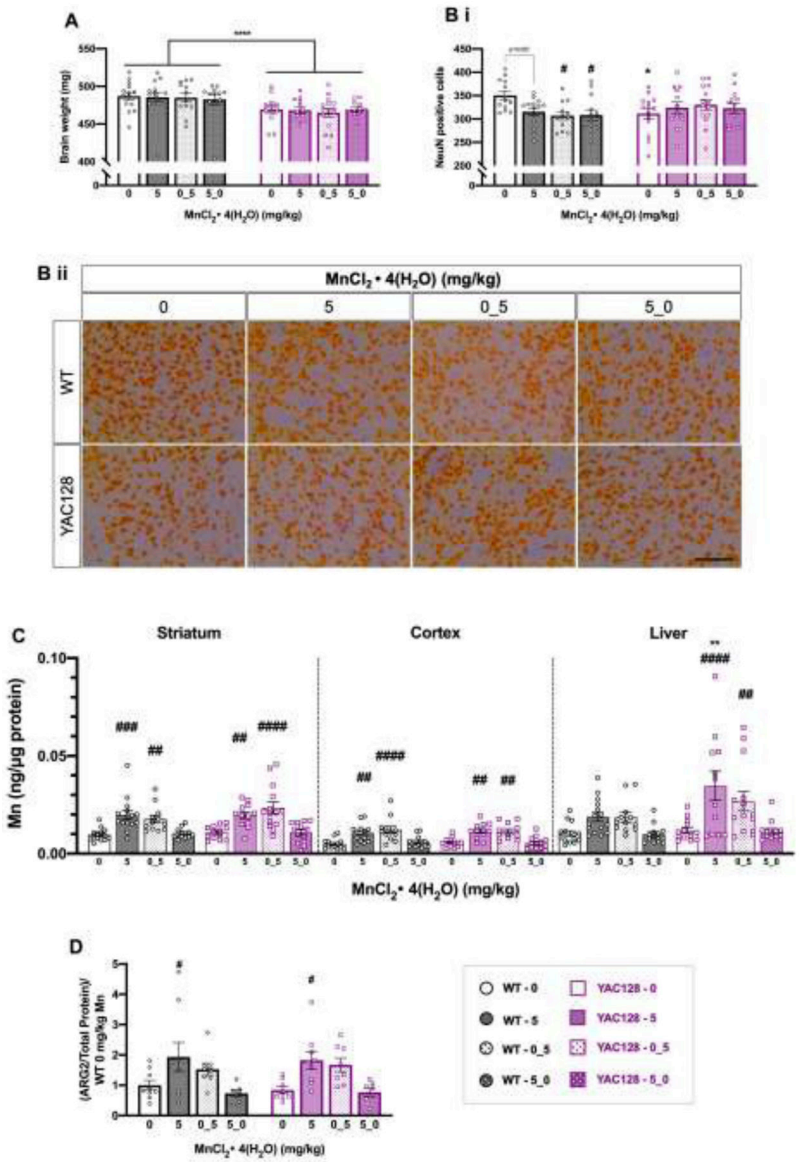

Figure 6.

Post-dissection outcomes for mice used in Study 2. **(A)** Total brain weights (mg). YAC128 mice weighed less than WT but there was no effect of Mn. **(B)** (i) YAC128 vehicle mice had a 10% decrease in density of NeuN positive cells compared to WT vehicle (*). Mn led to a significant decrease in NeuN positive cell density in the ”0_5” (p=0.015) and “5_0” groups (p=0.016) compared to WT vehicle (#), but NeuN positive cell density in YAC128 mice was unaffected by Mn treatment. (ii) Representative NeuN positive cells at 40x magnification. Scale bar = 200 µm. **(C)** Mn levels in striatum (left), cortex (middle) and hepatic (right) tissue for all genotypes and exposure groups. There was a significant increase in Mn levels in all three tissue types following exposure. A # symbol indicates significant difference from vehicle (0) within that genotype. In liver, there was a significant main effect of genotype, but post-hoc Sidak’s revealed that within Mn exposure groups, the only significant genotype difference was between YAC128 and WT that received the continuous 5 mg/kg Mn dose,

with accumulation being greater in YAC128 mice compared to WT. **(D)** ARG2 protein expression by western blot in the striata of a subset of mice from Study 2 (n=7-9 per genotype-treatment group). There was no significant effect of genotype, but Mn increased ARG2 expression. However, only the continuous 5 mg/kg Mn dose led to a significant increase in ARG2 compared to vehicle within each genotype. For all, mean ± S.E.M. plotted unless otherwise noted. Asterisks * indicate genotype effect, pound # indicates Mn effect within genotype. #/* p <0.05, **, p<0.01, *** p<0.001, **** p<0.0001. n=12-15 per genotype-treatment group with approximately equal number of males and females unless otherwise noted.